Influence of substrate temperature on titanium oxynitride thin films prepared by reactive sputtering

Chappé, J.M.; Martin, N.; Pierson, J.F.; Terwagne, Guy; Lintymer, J.; Gavoille, J.; Takadoum, J.

Published in:
Applied Surface Science

Publication date:
2004

Document Version
Peer reviewed version

Available online at www.sciencedirect.com
SCIENCE DIRECT®
Applied Surface Science 225 (2004) 29–38
applied surface science
www.elsevier.com/locate/apsusc

Influence of substrate temperature on titanium oxynitride thin films prepared by reactive sputtering

J.-M. Chappé[a,*], N. Martin[a], J.F. Pierson[b], G. Terwagne[c], J. Lintymer[a], J. Gavoille[a], J. Takadoum[a]

[a]*Laboratoire de Microanalyse des Surfaces (LMS), Ecole Nationale Supérieure de Mécanique et des Microtechniques (ENSMM), 26 Chemin de l'épitaphe, 25030 Besançon Cedex, France*
[b]*Centre de Recherche sur les Ecoulements, les Surfaces et les Transferts (CREST) UMR CNRS 6000, Université de Franche-Comté, Pôle Universitaire, BP 71427, 25211 Montbéliard Cedex, France*
[c]*Laboratoire d'Analyses par Réactions Nucléaires, Facultés Universitaires, Notre-Dame de la Paix, 61 Rue de Bruxelles, 5000 Namur, Belgium*

Received 16 July 2003; received in revised form 17 September 2003; accepted 17 September 2003

Abstract

Thin films of titanium oxynitride were successfully prepared by dc reactive magnetron sputtering using a titanium metallic target, argon, nitrogen and water vapour as reactive gases. The nitrogen partial pressure was kept constant during every deposition whereas that of the water vapour was systematically changed from 0 to 0.1 Pa. These films were made at room temperature (293 K) (set A) and at 673 K (set B). The study consisted in comparing the evolution of deposition parameters like target potential or deposition rate and physical properties of films for each set. Elemental composition measurements obtained by RBS and NRA revealed a reverse and continuous evolution of nitrogen and oxygen contents. Structure and morphology of the films were analysed by X-ray diffraction (XRD) and scanning electron microscopy (SEM). Films deposited at room temperature became amorphous with an increasing supply of water vapour. A higher substrate temperature led to significant changes of the crystallographic structure: from fcc TiN without water vapour to a mixture of anatase + rutile for large amount of water vapour. The optical transmittance spectra of the film/glass substrate system were measured in the visible region as a function of the water vapour pressure. For both sets A and B, optical transmittance was influenced by the water vapour partial pressure. Electrical conductivity measured against temperature was gradually modified from metallic ($\sigma_{300\,K} = 1.49 \times 10^4$ S m^{-1}) to semi-conducting behaviour ($\sigma_{300\,K} = 2.15$ S m^{-1}) with an increasing supply of the water vapour partial pressure. Moreover, coatings prepared at room temperature exhibited a surprising maximum of the electrical conductivity for a small amount of water vapour (set A). Such surprising evolution vanished for set B with a restricted range of conductivity from $\sigma_{300\,K} = 1.1 \times 10^5$ to 7×10^2 S m^{-1}.

PACS: 68.55.-a; 68.60.-p

Keywords: Reactive sputtering; Titanium oxynitride; Water vapour; High temperature

* Corresponding author. Tel.: +33-381-402764; fax: +33-381-402852.
E-mail address: jm.chappe@ens2m.fr (J.-M. Chappé).

0169-4332/$ – see front matter © 2003 Elsevier B.V. All rights reserved.
doi:10.1016/j.apsusc.2003.09.028

1. Introduction

There has been a great interest for the production of reactive sputtered metallic oxynitride thin films during the past few years. In particular, titanium oxynitride thin films have been extensively investigated because of their remarkable optical and electrical properties, mechanical behaviours and chemical stability. In recent studies [1–4], they revealed behaviours included between metallic TiN and semi-conducting TiO_2 compounds. Physical vapour deposition (PVD) was found to be a convenient deposition technique to prepare TiO_xN_y with a tuneable N/O ratio and consequently with a wide range of properties [5–8]. Reactive magnetron sputtering is specially an attractive way to synthesise these films and can be applied at various deposition temperatures. A titanium target sputtered in a mixed working gas ($O_2 + N_2$) [9,10] or the reactive gas pulsing technique [3,11] can be used to modify N/O ratio in the films.

In this work, we report on the influence of the substrate temperature on titanium oxynitride thin films prepared by dc reactive magnetron sputtering using argon, and nitrogen and water as reactive gases. A comparison is firstly made between deposition parameters of set A (293 K) and set B (673 K). Then the evolution of the chemical composition, crystallographic structure, morphology, and the optical and electrical properties of the whole range of films is discussed as a function of the substrate temperature. Results will be compared to the expectations given by literature like Thornton's model [12].

2. Experimental

A home-made high vacuum reactor with a 40 L volume was used to perform the depositions of titanium oxynitride thin films. An ultimate pressure of 10^{-5} Pa was obtained with a turbomolecular pump backed with a mechanical pump. The reactor is equipped with a circular planar and water cooled magnetron sputtering source. A metallic titanium target (purity 99.6%, 50 mm diameter) was dc sputtered with a constant current density $J_{Ti} = 51$ A m^{-2}. The substrates (glass from micro slides and (1 0 0) silicon wafers) were grounded and kept at a constant temperature $T_A = 293$ K (set A) or $T_B = 673$ K (set B) during the deposition. The target was located at a distance of 50 mm from the substrate. Substrates were ultrasonically cleaned with acetone and alcohol before each run. Before introducing nitrogen and water vapour, Ti target was pre-sputtered in a pure argon atmosphere for 5 min in order to remove the surface oxide layer and clean its surface. Argon and nitrogen partial pressures were maintained at 0.4 and 0.1 Pa, respectively, using mass flow controllers and a constant pumping speed $S = 24.7$ L s^{-1}. The water vapour partial pressure was derived by subtracting nitrogen and argon partial pressure from the total pressure (plasma on) [4] and was systematically changed from 0 to 0.1 Pa using a leak valve connected to a de-ionised water flask. The deposition time was adjusted in order to obtain a thickness close to 400 nm (measured by a Taylor Hobson mechanical profilometer). Substrates were heated from room temperature (set A) to 673 K (set B) thanks to a resistive heater which maintained the temperature within ±15 K.

The elemental analysis of all elements present in the coatings was performed combining Rutherford backscattering spectroscopy (RBS) and nuclear reaction analysis (NRA). In order to analyse the heavy element (Ti) in the coatings, a 2 MeV α particles beam used for the backscattering experiment was produced by the 2 MV Tandetron accelerator installed at LARN in Namur and the scattered particles were detected in a passivated implanted planar silicon (PIPS) detector placed at 165° relative to the incident beam. The analysis of light elements in the coatings was performed with a 5.2 MeV α particles beam produced with the same accelerator. The particles due to $^{14}N(\alpha, p_0)^{17}O$ and $^{14}N(\alpha, p_1)^{17}O$ nuclear reactions were detected in a PIPS detector placed at 90° relative to the incident beam. The α scattered particles were stopped in a 24 μm Mylar foil filter located in front of the detector. Simultaneously, the scattered α particles were detected in a PIPS detector at backward angle (165°). At this incident energy, the cross sections of the elastic (α, α) reaction on light elements are non-Rutherford. Data from the literature were used to take into account the true cross sections [13–15] in order to obtain realistic simulation of the experimental spectra. The crystallographic structure was investigated by X-ray diffraction (XRD) using monochromatised Cu Kα radiation at a grazing angle incidence $\theta = 1°$. Cross sectional scanning electron microscopy

(SEM) observations were performed on a JEOL JMS-6400F field emission SEM at an acceleration voltage of 5 kV. Optical properties were analysed from optical transmittance spectra of the film/glass substrate system recorded with a Lambda 20 UV-Vis Perkin-Elmer spectrophotometer. The electrical conductivity of the films deposited on glass substrates was measured as a function of temperature using the four probes method with the van der Pauw configuration.

3. Results and discussion

3.1. Process characteristics

Two phenomena are at stake to understand and explain the evolution of process characteristics for the coatings studied in this work. The first one is the typical feature of the reactive sputtering process [16] and the second one is due to presence of water vapour as reactive gas [4]. Their association allows detailing different phases in the behaviour of deposition rate (Fig. 1) and titanium target potential (Fig. 2). For set A, the deposition rate exhibits a continuous evolution from 151 to 48 nm h^{-1} when the water vapour pressure increases from 0 to 14 Pa. However, a maximum is reached for P_{H_2O} close to 5.0×10^{-2} Pa. Similar results have been obtained by Martin et al. [3] for the deposition of titanium oxynitride thin films by the reactive gas pulsing technique. The evolution of the deposition rate versus water vapour pressure can be explained by the occurrence of a competition phenomenon between the removal by sputtering of a nitride layer at the surface of the target and its substitution by an oxide one. At substrate temperature of 673 K (set B), the rate drop is shifted to lower P_{H_2O} values and maximum is less significant because of desorption phenomena of water, which is favoured at high substrate temperature (Fig. 1) [17]. This shift is due to the increasing reactivity of H_2O (especially oxygen) with deposited particles at 673 K, and occurs between the nitrided and oxidised sputtering mode. However, the amount of water vapour to avalanche the process in oxidised sputtering mode is nearly equivalent at 293 and 673 K (Fig. 2) because transition is between 0.01 and 0.1 Pa for both temperatures. In addition, measurements of the Ti target potential can be used to assess the poisoning effect of the target. Results for set B are similar to those of set A and show the three regions already studied by the authors [4], i.e. from nitrided sputtering mode (low water vapour pressure) to the oxidised one (high pressure) by mixed one corresponding to a high deposition rate. The only difference is the shift described above due to target

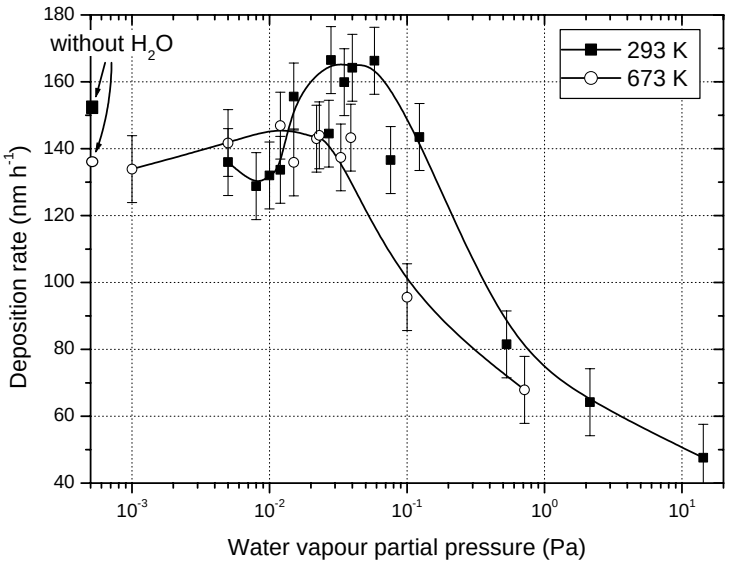

Fig. 1. Deposition rate of titanium oxynitride thin films vs. water vapour partial pressure at 293 K (set A) and 673 K (set B).

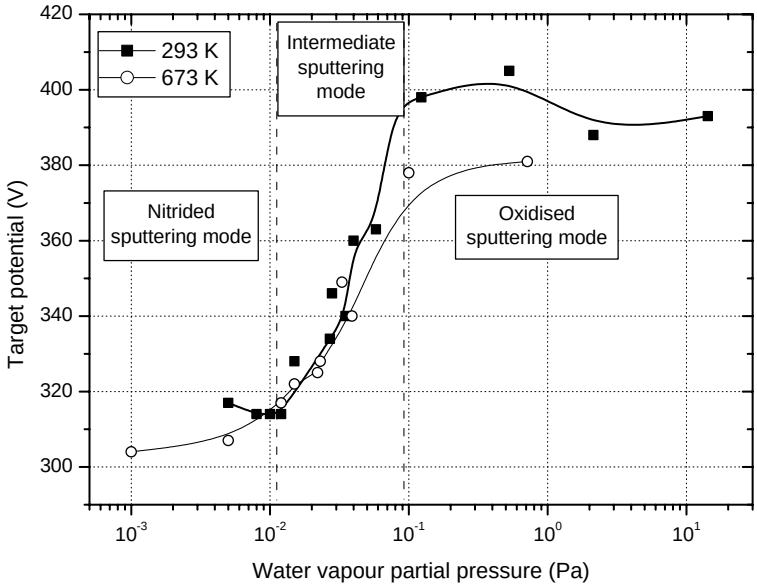

Fig. 2. Titanium target potential U_{Ti} as a function of the water vapour partial pressure at 293 K (set A) and 673 K (set B).

erosion and water desorption. As expected, the process characteristics are not modified by the high substrate temperature but mainly by the normal target erosion and supply of reactive gases.

3.2. Chemical composition, structure and morphology

Water vapour was used as a reactive gas to modulate the nitrogen and oxygen concentrations. Elemental composition measurements carried out by RBS and NRA for set A (Fig. 3a) show a reverse and continuous evolution of oxygen and nitrogen atomic compositions from $TiO_{0.15}N_{1.1}H_{0.07}$ at $P_{H_2O} = 0$ Pa to $TiO_{2.04}N_{0.19}H_{0.37}$ at $P_{H_2O} = 7.6 \times 10^{-2}$ Pa. In addition, a significant amount of hydrogen (higher than 10 at.%) is observed when P_{H_2O} reaches 7.6×10^{-2} Pa. Similar results were obtained by others [3,18–22] about this reverse evolution in metallic oxynitride coatings by simple variation of the oxygen partial pressure at room temperature. In spite of a very low supply of oxygen into the process (or water vapour in our case), an abrupt increase of the oxygen amount in oxynitride films is systematically measured mainly due to the strong reactivity of oxygen with metals. It remains valid for high substrate temperature (set B), as shown in Fig. 3b. It should be noted that the amount of oxygen in films deposited without water is strongly reduced when the substrate temperature is fixed at 673 K. At this temperature, the evolutions of oxygen and nitrogen atomic compositions are inverted while that of hydrogen remains lower than 8.5%. Coatings seem to trap less hydrogen at high temperature because of desorption. Moreover films revealing smaller grain sizes (TiO_xN_y) by XRD (see below) provide fewer sites, which are likely to keep hydrogen atoms. The association of these two phenomena (desorption and grain size decreasing) may explain the irregular shape of the films' hydrogen content curve.

For set A, X-ray diffraction patterns of the films deposited on (1 0 0) Si substrates show that the crystallographic structure is particularly influenced by low water vapour pressures (Fig. 4a). Without water and up to $P_{H_2O} = 8 \times 10^{-3}$ Pa, peaks corresponding to the fcc TiN phase appear with a preferential orientation along the (1 1 1) direction. This kind of nano-structured compound (the Scherrer's method revealed a crystallite size about 20 nm) commonly observed by others [23–25] disappears when water vapour pressure exceeds 8.0×10^{-3} Pa. TiN:O coatings lose their orange-brownish colours and become TiO_xN_y with a dark green colour and patterns exhibiting peaks

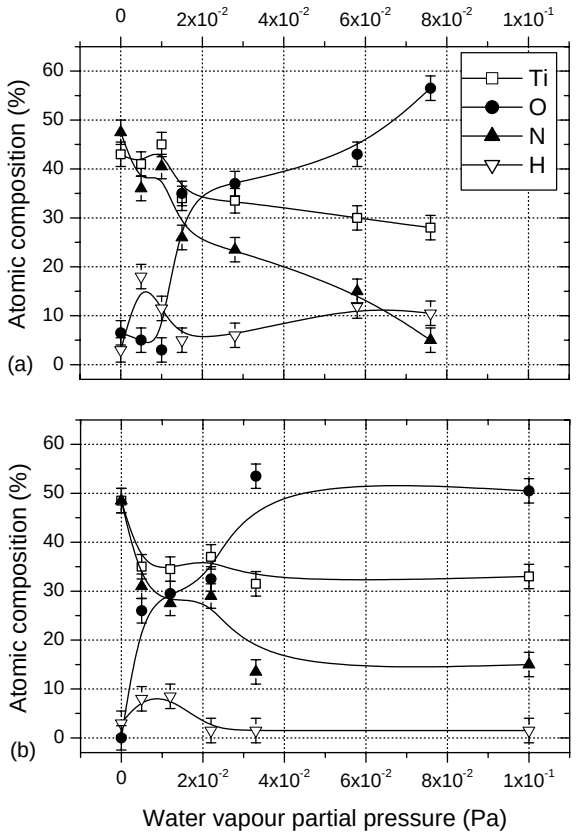

Fig. 3. Influence of the water vapour partial pressure on the chemical composition of titanium oxynitride thin films deposited at (a) 293 K (set A) and (b) 673 K (set B). A reverse evolution of oxygen and nitrogen concentrations can be noticed for both sets.

corresponding to fcc structure. Since TiO and TiN exhibit the same crystallographic structure (fcc) with neighbour lattice parameter ($a_{TiN} = 0.424$ nm and $a_{TiO} = 0.419$ nm), X-ray diffraction is not a suitable method to distinguish between these two structures. Since the diffraction peaks of the oxynitride films are located between those of TiO and TiN, a progressive substitution of nitrogen atoms by oxygen ones may occur when the water vapour partial pressure increases. However, this behaviour is not consistent with the chemical composition of the deposited films. Indeed when $P_{H_2O} = 2.7 \times 10^{-2}$ Pa, the atomic ratio (O + N)/Ti is close to 1.81 (Fig. 3a). Thus, the right structure of TiO_xN_y thin film can not be clearly identified. The films may be biphased: a weakly crystallised fcc phase and an amorphous one. When the water vapour pressure is higher than 1.2×10^{-1} Pa, the films become transparent (TiO_2:N) and exhibit an amorphous structure. The loss of a long range order with a high amount of water vapour is due to a low surface diffusion of the particles impinging on the substrate or the growing film (because of low substrate temperature), and to the growth competition between titanium nitride and titanium oxide phases on the growing film. Results for sets A are consistent with those found by Bittar et al. [18] and later by Ianno et al. [10] about aluminium oxynitride coatings. They claimed that an addition of small amounts of oxygen in the feed gas during deposition prevents the formation of a crystalline structure. Set B is supposed to include films presenting better crystallised structures (Fig. 4b). With low water vapour partial pressure, TiN films prepared at 673 K do not exhibit a preferential orientation along the (1 1 1) direction as previously observed for set A. A higher substrate temperature favours surface diffusion of sputtered particles and then reduces texture. For water vapour partial pressures higher than 5.0×10^{-3} Pa and up to 2.2×10^{-2} Pa, diffracted signals correspond to crystallised fcc structure as recorded for set A but for a shorter range of pressures (occurrence of fcc phase for $P_{H_2O} \leq 2.7 \times 10^{-2}$ Pa for set A). This is due to the reactivity of titanium towards oxygen which rises with temperature. Therefore, deposition of fcc phase is enhanced but its boundaries are shifted to lower water vapour partial pressures as temperature increases. Furthermore, it appears clearly in Fig. 4b that the full width at half maximum of the diffraction peak increases with the water partial pressure indicating a refinement of the grain size. This refinement corresponds to an amorphisation of the deposited films when P_{H_2O} is higher than 3.3×10^{-2} Pa. Here again, the occurrence of the amorphous structure is moved to lower water vapour partial pressures compared to set A and for a narrow window. Results for set B reveal interesting X-ray diffraction patterns for TiO_2:N (Fig. 4b). Indeed, at high substrate temperature, they exhibit several peaks corresponding to anatase and rutile phases (approximately same number). According to Exharos [26] and Löbl et al. [27], 673 K is too low to obtain a large amount of rutile phase. Martin [28] indicates that the energy of the particles impinging on substrate is high enough to form an anatase/rutile mixture by magnetron sputtering (energy of sputtered particles included

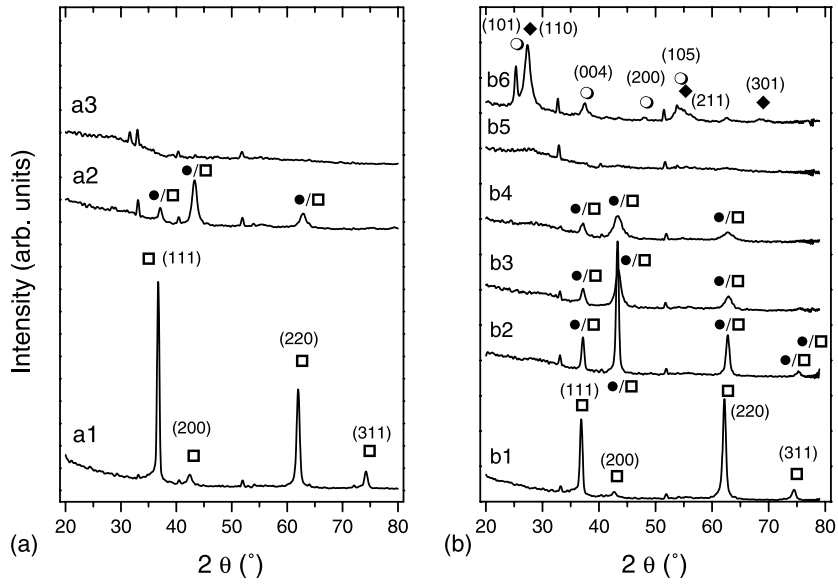

Fig. 4. X-ray diffraction patterns of titanium oxynitride thin films deposited on (1 0 0) silicon wafers at (a) 293 K (set A): (a1) $P_{H_2O} = 8.0 \times 10^{-3}$ Pa, (a2) $P_{H_2O} = 2.7 \times 10^{-2}$ Pa, and (a3) $P_{H_2O} = 1.23 \times 10^{-1}$ Pa; (b) 673 K (set B): (b1) $P_{H_2O} = 1.0 \times 10^{-3}$ Pa, (b2) $P_{H_2O} = 5.0 \times 10^{-3}$ Pa, (b3) $P_{H_2O} = 1.2 \times 10^{-2}$ Pa, (b4) $P_{H_2O} = 2.2 \times 10^{-2}$ Pa, (b5) $P_{H_2O} = 3.3 \times 10^{-2}$ Pa, and (b6) $P_{H_2O} = 1.0 \times 10^{-1}$ Pa. (□) TiN; (●) TiO; (◆) Rutile; (○) Anatase.

between 1 and 10 eV). This energy assessment is consistent with investigations from Wei et al. [29] in case of dc glow discharge.

SEM images of the cross section of the films systematically show a typical columnar microstructure (Fig. 5) for both sets. From melting points of TiN and TiO_2 ($mp_{TiN} = 3223$ K and $mp_{TiO_2} = 2113$ K, respectively), the temperature ratio ($T_{substrate}/T_{mp}$) is lower than 0.13 for set A and included between 0.21 (TiN) and 0.33 (TiO_2) for set B. According to the Thornton's structure zone model [12], set A micrographs correspond to zone 1 and set B ones to zone T (transition zone). For set A, films are formed by narrow vertical grains with a densely packed fibrous morphology. Surface diffusion phenomena are not able to develop in this zone due to little adatom surface mobility. Films from set B exhibit fibrous grains, which are longer than that observed for set A and closer to a columnar aspect. Such microstructure tends to zone 2 of the Thornton's structure zone model. SEM micrographs also show that adhesion of the films to the silicon substrate significantly depends on the water vapour pressure and the substrate temperature. At room temperature, a clear detachment of the coating is observed for TiN:O films (Fig. 5a1) while adhesion to the surface of the Si substrate seems to be improved for titanium oxynitride (Fig. 5a2) and is even better for TiO_2:N films (Fig. 5a3) since the fracture of silicon wafer is extended into the coating. Micrographs from set B do not allow drawing the same conclusions. No film deposited at 673 K shows a clear detachment away from the Si substrate. In addition, TiO_xN_y film (Fig. 5b2) presents signs of good adhesion to the substrate: some fractures can be noticed from the substrate to the coating through a (around 50 nm) thick interface. Such observations support an enhancement of the TiO_xN_y thin film adhesion to the silicon substrate at 673 K. As a result, the surface diffusion of sputtered particles is improved at high temperature. This favours reactivity of adatoms with the surface of the substrate and leads to a better adhesion of the films.

3.3. Optical and electrical properties

By depositing at high temperature, optical properties like refractive index or optical transmittance of the films are also modified. The optical transmittance

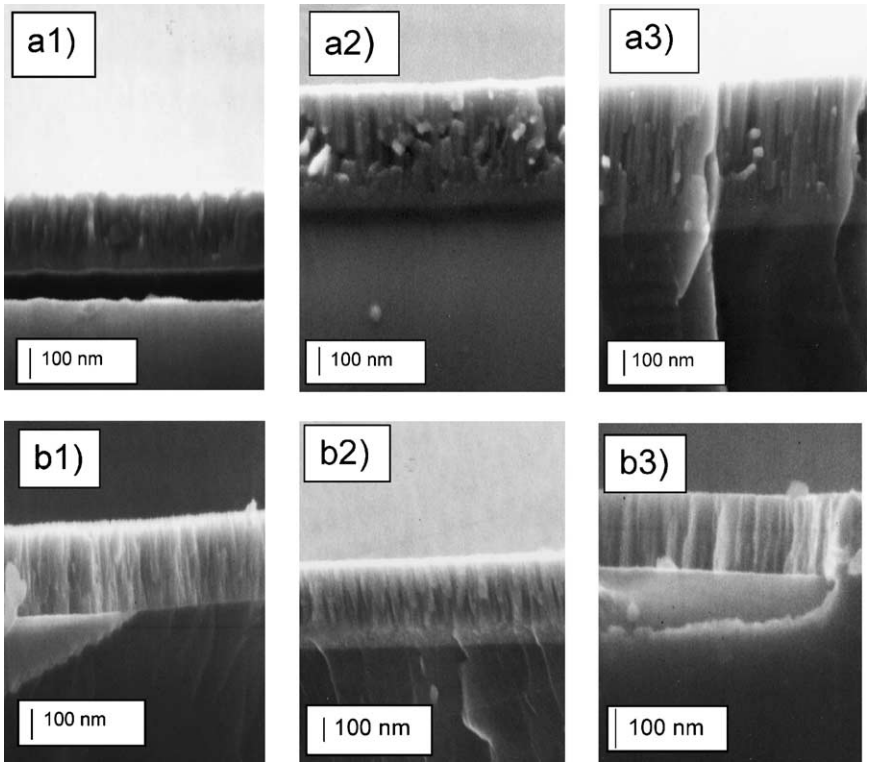

Fig. 5. Cross section observations by SEM of titanium nitride, oxynitride and oxide thin films prepared with different water vapour partial pressures at 293 K (set A): (a1) $P_{H_2O} = 0$ Pa, (a2) $P_{H_2O} = 4.0 \times 10^{-2}$ Pa, and (a3) $P_{H_2O} = 1.2 \times 10^{-1}$ Pa; 673 K (set B): (b1) $P_{H_2O} = 0$ Pa, (b2) $P_{H_2O} = 2.8 \times 10^{-2}$ Pa, and (b3) $P_{H_2O} = 1.82$ Pa. A columnar microstructure is systematically observed.

spectra of the film/glass substrate system for samples from sets A and B are shown in Fig. 6. The three regions previously described [4] (TiN:O; TiO_xN_y; TiO_2:N) appear for both sets. For low water vapour partial pressures ($P_{H_2O} < 2.8 \times 10^{-2}$ Pa), spectra of TiN:O coatings are almost completely absorbent. For moderated pressures (3.3×10^{-2} Pa $< P_{H_2O} < 5.8 \times 10^{-2}$ Pa) films are slightly transparent and exhibit a dark green colours aspect specific to titanium oxynitride materials and for higher values ($P_{H_2O} > 5.8 \times 10^{-2}$ Pa) TiO_2:N films are transparent. Typical interference fringes are observed for sets A and B. The average transmittance at 600 nm as a function of the water vapour partial pressure is represented in Fig. 7 for both sets. Such a figure clearly illustrates an abrupt increase of the transmittance from 0 to 75–80% when the water vapour partial pressure changes from 2×10^{-2} to 6×10^{-2} Pa. This range of pressure correlates with those determined by XRD and support again the three kinds of regions previously suggested. These results also support the gradual transition of the optical behaviours from metallic TiN to insulating TiO_2 compound.

Electrical conductivity (σ) measured at room temperature (set A) for various water vapour pressures (Fig. 8) corroborates with optical results and process analyses. For a water vapour pressure included between 8×10^{-3} and 1.2×10^{-2} Pa, electrical conductivity of the films is enhanced and reaches a maximum value $\sigma_A = 3.8 \times 10^5$ S m^{-1} close to $P_{H_2O} = 10^{-2}$ Pa while it remains next to 10^4 S m^{-1} for lower water vapour pressure (TiN:O). It correlates with an increase of the target potential, a large increase of the oxygen concentration in the films and with a colour change from orange brownish to a metallic dark green aspect. Then the electrical conductivity is monotonously reduced down to 2.6 S m^{-1} as water vapour pressure increases from

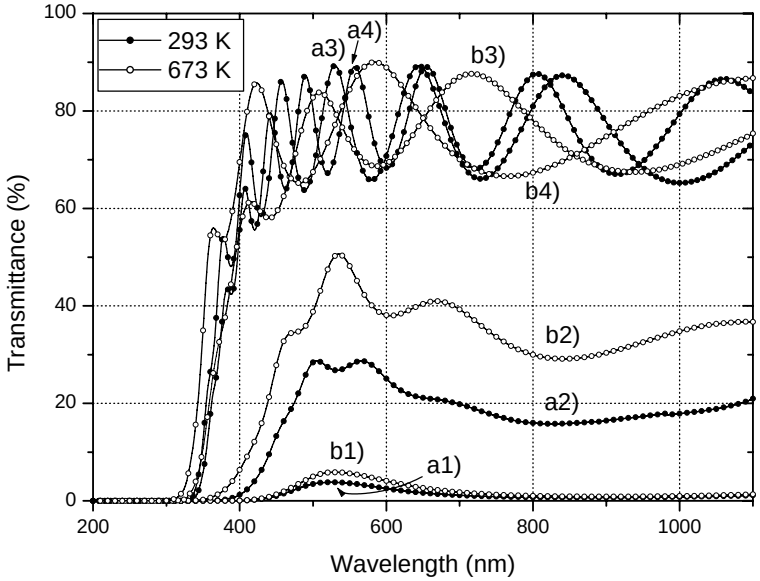

Fig. 6. Transmittance spectra in the visible region of titanium oxynitrides deposited on glass substrates at 293 K (set A): (a1) $P_{H_2O} = 2.8 \times 10^{-2}$ Pa, (a2) $P_{H_2O} = 4.0 \times 10^{-2}$ Pa, (a3) $P_{H_2O} = 7.6 \times 10^{-2}$ Pa, and (a4) $P_{H_2O} = 1.23 \times 10^{-1}$ Pa; 673 K (set B): (b1) $P_{H_2O} = 2.3 \times 10^{-2}$ Pa, (b2) $P_{H_2O} = 3.9 \times 10^{-2}$ Pa, (b3) $P_{H_2O} = 4.0 \times 10^{-2}$ Pa, and (b4) $P_{H_2O} = 1.2 \times 10^{-1}$ Pa.

10^{-2} to 7.6×10^{-2} Pa, because of the increasing oxygen content in the films and thus the increasing semi-conducting behaviour. The gradual transition from metallic to this behaviour is also observed from electrical conductivity measurements versus temperature (Table 1). Activation energy "E_a" is calculated assuming a linear behaviour in an Arrhenius plot of the conductivity as a function of the reverse temperature.

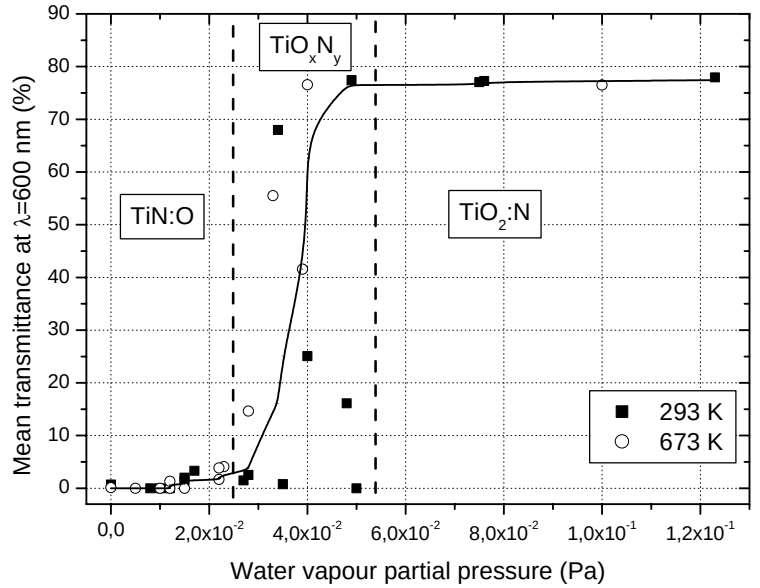

Fig. 7. Mean transmittance at 600 nm of titanium oxynitrides deposited at 293 K (set A) and 673 K (set B) on glass substrates.

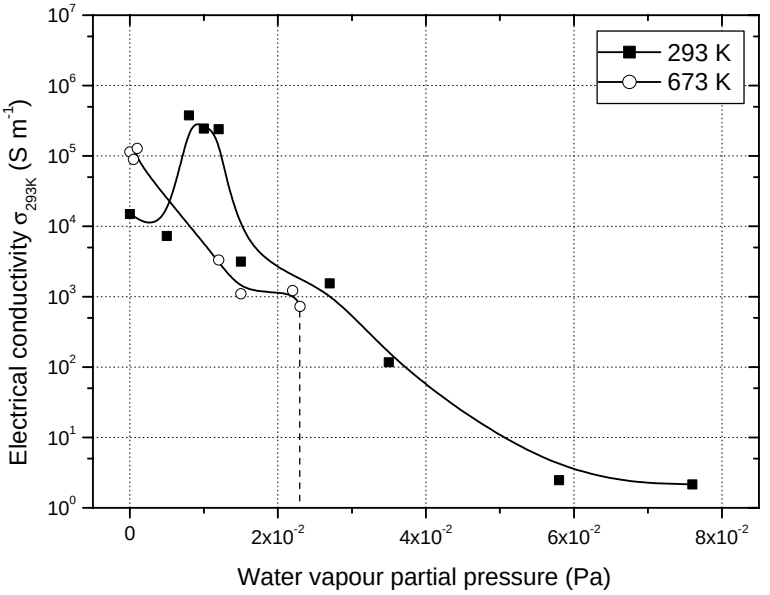

Fig. 8. Electrical conductivity σ at 300 K of titanium nitride and oxynitride thin films deposited at 293 K (set A) and 673 K (set B) vs. water vapour partial pressure (doted line corresponds to a very low conductivity that cannot be measured using the van der Pauw configuration).

E_a increases from 7 meV ($P_{H_2O} = 10^{-2}$ Pa) to 199 meV ($P_{H_2O} = 5.8 \times 10^{-2}$ Pa) and also corresponds to the reverse evolution of oxygen and nitrogen concentrations in the films.

In addition, a continuous decrease of σ measured versus water vapour supply into the process or oxygen in the films [3,18,30] is commonly measured as similarly observed for set B (Fig. 8). Indeed the range of conductivity of films deposited at 673 K is more restricted and is included between 10^5 and 10^3 S m^{-1} for a narrow range of water vapour partial pressures. Electrical conductivity cannot be measured by the van der Pauw method for P_{H_2O} higher than 2.3×10^{-2} Pa. It is worth noting that the metal/semi-conducting transition for set B occurs at weaker water vapour partial pressures compared to set A. This is probably due to the greater reactivity of titanium with oxygen at 673 K than at room temperature. Moreover, the decrease of electrical conductivity is smooth. Maximum of electrical conductivity observed close to $P_{H_2O} = 10^{-2}$ Pa for set A vanishes and correlates with the phase occurrence and crystallographic structure (as previously discussed). Values for E_a corresponding to negative slope lines are included between 11 meV ($P_{H_2O} = 5 \times 10^{-3}$ Pa) and 96 meV ($P_{H_2O} = 2.3 \times 10^{-2}$ Pa) (Table 1).

Table 1
Activation energy E_a (linear behaviour in the Arrhenius plot measured between 300 and 473 K) of the electrical conductivity as a function of water vapour partial pressure of titanium oxynitride thin films deposited at 293 and 673 K

Substrate temperature (K)	P_{H_2O} (Pa)	E_a (meV)
293 (set A)	0.0	–
	1.0×10^{-2}	7
	1.5×10^{-2}	73
	3.5×10^{-2}	112
	5.8×10^{-2}	199
673 (set B)	1.0×10^{-3}	–
	5.0×10^{-3}	11
	1.2×10^{-2}	35
	2.2×10^{-2}	79
	2.3×10^{-2}	96

4. Conclusion

Oxynitride thin films have been successfully deposited by dc reactive magnetron sputtering with water vapour as reactive gas. The effect of high substrate

temperature on process characteristics and physical properties of the films has been investigated. Deposition rate and target potential have not been influenced by the substrate temperature even at 673 K. Nevertheless, experimental parameters have been taken into account to determine three types of operating conditions suitable to deposit titanium nitride (TiN:O), titanium oxynitride (TiO_xN_y) and titanium dioxide thin films (TiO_2:N) with various metalloid concentrations. At high temperature, and with an increase of the water vapour supply into the process, films exhibited peaks corresponding to TiN, fcc (TiO and/or TiN) and anatase/rutile phases, respectively. Evolutions of oxygen and nitrogen atomic compositions are inverted for both sets while the hydrogen one becomes significant at high water vapour partial pressure. Optical transmittance of the films from sets A and B showed similar evolution and corroborated the occurrence of the three types of structure: TiN:O; TiO_xN_y; TiO_2:N versus water vapour partial pressure. It is worth noting the vanishing of the electrical conductivity maximum for intermediate water vapour partial pressures at high substrate temperature. SEM micrographs were in agreement with the Thornton's structure zone model and results for set B showed slight differences about physical properties but did not allow quantifying precisely a shift of the region boundaries. The right structure of titanium oxynitride compounds versus oxygen/water supply and substrate temperature still remains an open question. Further investigations are required to suggest a phase occurrence zone model.

Acknowledgements

The authors are grateful to R. Guinchard for technical support and they acknowledge C. Millot for experimental assistance during SEM observations. They thank Region of Franche-Comté for financial support.

References

[1] M.J. Jung, K.H. Nam, Y.M. Chung, J.H. Boo, J.G. Han, Surf. Coat. Technol. 171 (2003) 71.
[2] F. Fabreguette, L. Imhoff, M. Maglione, B. Domenichini, M.C. Marco de Lucas, P. Sibillot, S. Bourgeois, M. Sacilotti, Chem. Vap. Deposition 6 (2000) 1.
[3] N. Martin, O. Banakh, A.M.E. Santo, S. Springer, R. Sanjinés, J. Takadoum, F. Lévy, Appl. Surf. Sci. 185 (2001) 123.
[4] J.-M. Chappé, N. Martin, G. Terwagne, J. Lintymer, J. Gavoille, J. Takadoum, Thin Solid Films 440 (2003) 66.
[5] T.E. Plowman, M.D. Garrison, D.S. Walker, W.M. Reichert, Thin Solid Films 243 (1994) 610.
[6] M. Suzuki, Y. Saito, Appl. Surf. Sci. 173 (2001) 171.
[7] W.L. Scopel, M.C.A. Fantini, M.I. Alayo, I. Pereyra, Thin Solid Films 413 (2002) 59.
[8] M.H. Kazemeini, A.A. Berezin, N. Fukuhara, Thin Solid Films 372 (2000) 70.
[9] T. Oyama, H. Ohsaki, Y. Tachibana, Y. Hayashi, Y. Ono, N. Horie, Thin Solid Films 351 (1999) 235.
[10] N.J. Ianno, H. Enshashy, R.O. Dillon, Surf. Coat. Technol. 155 (2002) 130.
[11] N. Martin, R. Sanjinés, J. Takadoum, F. Lévy, Surf. Coat. Technol. 142–144 (2001) 615.
[12] J.A. Thornton, J. Vac. Sci. Technol. 11 (1974) 666.
[13] F. Ye, Z. Zhuying, Z. Guoqing, Y. Fujia, Nucl. Instrum. Methods B94 (1994) 11.
[14] Z.S. Zheng, J.R. Liu, X.T. Cui, W.K. Chu, Nucl. Instrum. Methods B118 (1996) 214.
[15] G. Terwagne, J. Colaux, G.A. Collins, F. Bodart, Thin Solid Films 377–378 (2000) 441.
[16] W.D. Westwood, Phys. Thin Films 14 (1989) 1.
[17] J.E. Mahan, Physical Vapor Deposition of Thin Films, Wiley, New York, 2000, p. 97.
[18] A. Bittar, D. Cochrane, S. Caughley, J. Vac. Sci. Technol. A15 (1997) 223.
[19] M. Futsuhara, K. Yoshioka, O. Takai, Thin Solid Films 317 (1998) 322.
[20] A. Von Richthofen, R. Domnick, R. Cremer, D. Neuschütz, Thin Solid Films 317 (1998) 282.
[21] T. Suzuki, H. Saito, M. Hirai, H. Suematsu, W. Jiang, K. Yatsui, Thin Solid Films 407 (2002) 118.
[22] Y.G. Shen, Y.W. Mai, Mater. Sci. Eng. B95 (2002) 222.
[23] S. Groudeva-Zotova, R. Kaltofen, T. Sebald, Surf. Coat. Technol. 127 (2000) 144.
[24] K. Tominaga, S. Inoue, R.P. Howson, K. Kusaka, T. Hanabusa, Thin Solid Films 281–282 (1996) 182.
[25] O. Knotek, W.D. Münz, T. Leyendecker, J. Vac. Sci. Technol. A5 (1987) 2173.
[26] G.J. Exharos, J. Vac. Sci. Technol. A4 (1986) 2962.
[27] P. Löbl, M. Huppertz, D. Mergel, Thin Solid Films 251 (1994) 72.
[28] N. Martin, Ph.D. Thesis #620, University of Franche-Comté, France, 1997.
[29] H. Wei, Z. Liu, K. Yao, Vacuum 57 (2000) 87.
[30] J. Guillot, F. Fabreguette, L. Imhoff, O. Heintz, M.C. Marco de Lucas, M. Sacilotti, B. Domenichini, S. Bourgeois, Appl. Surf. Sci. 177 (2001) 268.